

Coulomb scattering in plasma revised

S. Gordienko

*L.D.Landau Institute for Theoretical Physics, Russian Academy of Science, Kosigin St. 2, Moscow, Russia**

D.V. Fisher

Faculty of Physics, Weizmann Institute of Science - Rehovot 76100, Israel†

J. Meyer-ter-Vehn

Max-Planck-Institut für Quantenoptik - D-85748 Garching, Germany‡

(Dated: November 15, 2018)

A closed expression for the momentum evolution of a test particle in weakly-coupled plasma is derived, starting from quantum many particle theory. The particle scatters from charge fluctuations in the plasma rather than in a sequence of independent binary collisions. Contrary to general belief, Bohr's (rather than Bethe's) Coulomb logarithm is the relevant one in most plasma applications. A power-law tail in the distribution function is confirmed by molecular dynamics simulation.

PACS numbers: 52.40.Mj,03.65.Nk,52.65.Yy

Though Coulomb scattering is a most basic process in plasma and has been studied for a century [1], doubts concerning the treatment as a sequence of independent binary collisions remained [2, 3], and recent analysis [4] has revealed that this standard assumption is not justified in general and requires revision. Here we derive the time-dependent many-particle wavefunction of a test particle simultaneously interacting with N particles residing in the Debye sphere. The plasma parameter $N = n\lambda^3 > 1$ involves the plasma density n and the screening length $\lambda = \max(v_T/\omega_p, v_0/\omega_p)$, where v_T is the thermal velocity of electrons, v_0 the velocity of the test particle, and $\omega_p = \sqrt{4\pi ne^2/m_e}$ the plasma frequency. We emphasize that the collective interaction described here is different and in addition to Debye screening; it is not included in the usual dielectric approach [5]. The new results can be viewed as interaction of the test particle with the charge fluctuations inside the Debye sphere; in this picture, the test particle of charge Z_0e is scattered by an effective, spatially extended charge $e\sqrt{N}$ rather than by a sequence of binary collisions.

This has deep consequences for the Coulomb logarithm, because it drastically shifts the borderline between classical and quantum Coulomb scattering, extending the domain in which the classical approximation applies. This is shown in Fig. 1. In the binary collision approach (Fig. 1a), the borderline is given by the parameter $\alpha = Z_0e^2/\hbar v_0$ such that $\alpha < 1$ defines the quantum-mechanical region where the Born approximation leads to Bethe's logarithm $L_q = \ln(\lambda m_e v_0/\hbar)$ [6], while for $\alpha > 1$ classical mechanics apply leading to Bohr's logarithm $L_{cl} = \ln(\lambda m_e v_0^2/Z_0e^2)$. In the present theory instead, the borderline is given by $\alpha N^{1/2} \approx 1$,

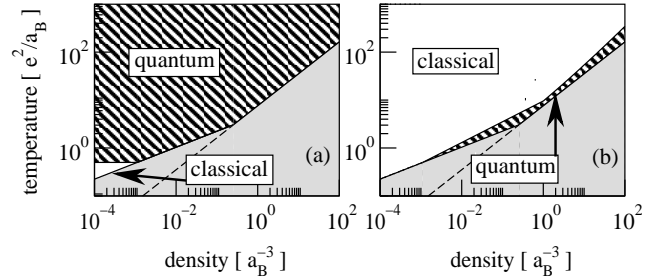


FIG. 1: Regions in a density-temperature plane (atomic units) in which Bohr's classical Coulomb logarithm (white area) and Bethe's quantum expression (hatched area) apply; (a) binary collision theory with borderline defined by $\alpha = Z_0e^2/\hbar v_0 = 1$, and (b) present theory with approximate separation along $\alpha^2 N(1 + \ln N) = 1$. Also shown as grey area are the region of strongly non-ideal plasma (borderline: $T \sim n^{1/3}$) and the region of degenerate plasma (borderline: $T \sim n^{2/3}$).

and this leads to a very different picture in Fig.1b. Now L_{cl} applies to almost the entire high-temperature region, including e.g. the important domain of magnetic fusion plasmas, while L_q plays only a marginal role.

Let us first discuss this result in qualitative terms. A particular feature of the Coulomb ($1/r$) interaction is of crucial importance in this case, namely that scattering does not depend on α and \hbar , as we know from the Rutherford cross section. The difference between $\alpha < 1$ and $\alpha > 1$ regions arises only when the potential deviates from $1/r$, as it is the case in a plasma due to Debye screening occurring at long distances λ . This means the distinction between classical and quantum treatment reveals itself for small-angle scattering, while close collisions with large-angle scatter are not affected. This point has been emphasized strongly by Bohr (see p.448 in [1]) and also in Sivukhin's review [3] (p. 109–113). In accordance with Bohr "any attempt to attribute the difference

*Electronic address: gord@itp.ac.ru

†Electronic address: fndima@plasma-gate.weizmann.ac.il

‡Electronic address: meyer-ter-vehn@mpq.mpg.de

between [the classical $\alpha \gg 1$ and quantum $\alpha \ll 1$ cases] to the obvious failure of [the classical] pictures in accounting for collisions with an impact parameter smaller than [the de Broglie wave-length] will be entirely irrelevant. In fact, this argument would imply a difference between two distribution for the large angle scattering, while the actual differences occur only in the limits of small angles."

Now let us compare the classical scattering angle $\delta_{cl} = (Z_0 e e_* / m_0 v_0^2) / \lambda$ at distance λ with that of quantum diffraction $\delta_q = (\hbar / m_0 v_0) / \lambda$ [7]. The open question here concerns the effective net charge e_* which the test particle experiences when passing the Debye sphere. The value of e_* is not evident, because we are dealing with Coulomb collisions at distances much larger than $1/n^{1/3}$. The binary collision approximation circumvents this predicament by alleging that the total scattering can be treated as the sum of independent binary interactions happening at different times [3]. One is then led to take $e_* = e$ for granted instead of actually calculating e_* . The central result of this paper will be that the effective charge is essentially given by $e_* \approx e N^{1/2}$. The matching condition then is $\delta_{cl} / \delta_q \approx \alpha N^{1/2} \approx 1$ replacing the condition $\alpha \approx 1$ obtained in binary collision approximation [3]. The theory underlying Fig. 1b will now be derived. As a central result, we also present molecular dynamics simulations confirming the analytic theory.

The present analysis starts from a full quantum-mechanical description of the plasma in terms of the many-particle wave-function $\psi = \exp(iS/\hbar)$. The action function S satisfies the equation

$$-\frac{\partial S}{\partial t} = \sum_j \left(\frac{(\nabla_j S)^2}{2m_j} + \sum_{k>j} U_{j,k} - i\hbar \frac{\Delta_j S}{2m_j} \right), \quad (1)$$

where the indices j and k denote plasma particles for $j, k = 1, 2, 3 \dots$ and the test particle for $j, k = 0$, m_j are the masses, and $U_{j,k}$ represent the Coulomb interactions. Eq. (1) is equivalent to the exact Schrödinger equation and has the form of a Hamilton-Jacoby equation with additional terms that are proportional to \hbar and describe quantum effects. We examine the solution of Eq. (1) for the particular initial conditions $S(t=0) = \sum_{j \geq 0} \mathbf{p}_j \cdot \mathbf{r}_j$, (the Green function for the coordinate-momentum representation), where \mathbf{p}_j are given momenta of the plasma particles at $t=0$, and introduce

$$\sigma = S - \sum_{j \geq 0} (\mathbf{p}_j \cdot \mathbf{r}_j - \mathbf{p}_j^2 t / 2m_j)$$

such that $\sigma(t=0) = 0$. Now the clue for solving Eq.(1) is the high-energy approximation [7] which applies to an almost ideal plasma and requires $|\mathbf{p}_j| \gg |\nabla_j \sigma|$. Under this approximation we find

$$-\frac{\partial \sigma}{\partial t} = \sum_j \left(\mathbf{v}_j \cdot \nabla_j \sigma + \sum_{k>j} U_{j,k} - i\hbar \frac{\Delta_j \sigma}{2m_j} \right), \quad (2)$$

where $\mathbf{v}_j = \mathbf{p}_j / m_j$. The solution of Eq. (2) for $\sigma(t=0) = 0$ is

$$\sigma = - \sum_{j \geq 0} \sum_{k > j} \int_0^t U_{k,j}(\mathbf{D}_{k,j}) d\tau, \quad (3)$$

where $\delta \mathbf{r}_{k,j} = \mathbf{r}_k - \mathbf{r}_j$, $\delta \mathbf{v}_{k,j} = \mathbf{v}_k - \mathbf{v}_j$ and $\mathbf{D}_{k,j} = \delta \mathbf{r}_{k,j} - \delta \mathbf{v}_{k,j}(t - \tau)$. It can be verified by direct insertion. The terms $\Delta_j \sigma$ proportional to \hbar vanish for the special case of Coulomb $U \propto 1/|\mathbf{D}|$ interactions for distances $|\mathbf{D}| > 0$.

The problem of solution (3) is that it contains the singularities of $U_{k,j}(\mathbf{D}_{k,j})$ for close encounters with $|\mathbf{D}_{k,j}| \rightarrow 0$. This deficiency is due to the high energy approximation. Inserting Eq. (3) into $|\mathbf{p}_j| \gg |\nabla_j \sigma|$, we find that this condition is fulfilled only for regions

$$|\mathbf{D}_{k,j}| > |e_j e_k| / (\mu_{k,j} |\delta \mathbf{v}_{k,j}|^2) \quad (4)$$

with $0 < \tau < t$ and $\mu_{k,j} = m_j m_k / (m_j + m_k)$. Had we solved the nonlinear equation (1) exactly, we had obtained a non-singular result with the maximum momentum transfer of $2\delta v_{j,k} \mu_{j,k}$, as we know from Rutherford scattering. The way to deal with this problem is to cut out in the wavefunction those spatial regions which do not satisfy Eq. (4). The cut-off (4) warrants that the maximum momentum transfer $2\delta v_{j,k} \mu_{j,k}$ is preserved; this can be verified by operating with $-i\hbar \nabla_j$ on $\exp(iS/\hbar)$. It should be understood that this short-range cut-off is a technical correction (compare with [1], p. 448-449: "... the central region of the field... which, on classical mechanics, is responsible for all large angle scattering will, for $\alpha \ll 1, \dots$ gives rise to only a fraction of the order α^4 of the Rutherford scattering"). It has nothing in common with differences between classical and quantum scattering. These reveal themselves only at long ranges [1, 3]. Another detail concerning the general wavefunction concerns the initial conditions. In case the initial state of the plasma is defined by the wavefunction $\phi(t=0, \mathbf{p}_1, \mathbf{p}_2, \dots)$ rather than by a fixed set of momenta, the corresponding general wavefunction is given by

$$\psi(t, \mathbf{r}_0, \mathbf{r}_1, \dots) = \int \exp(iS/\hbar) \phi(t=0, \mathbf{p}_1, \mathbf{p}_2, \dots) \prod_{k \geq 1} d\mathbf{p}_k.$$

As it turns out, the explicit form of ϕ is of no relevance in the applications discussed below.

We now have at our disposal in analytical form the time-dependent many-particle wavefunction describing a dilute high-temperature plasma. This is a remarkable result. An outstanding feature is that it describes simultaneous multiple Coulomb interactions between the particles and, in this respect, goes beyond the binary collision approximation. Another essential property is that it holds for both the quasi-classical regime ($\sigma \gg \hbar$) as well as the deeply quantum-mechanical regime ($\sigma \ll \hbar$) and therefore provides a unique tool to investigate the transitional region. We now proceed to use this wavefunction

to calculate plasma properties. This is straightforward, though tedious, and therefore we can give here only the main results, leaving technical derivations to a separate publication.

We first consider the distribution function $M(t, \mathbf{Q})$ of transverse momentum \mathbf{Q} of a test particle moving at time $t = 0$ with momentum \mathbf{p} collinear to the x -axis. For brevity we consider a fast ion $m_0 \gg m_e$, $v_0 \gg v_T$ for times that are longer than $t_0 = \lambda/v_0$, though shorter than the collision time $t_c \sim m_0 N t_0 / m_e L_{cl,q}$. $M(t, \mathbf{Q})$ is obtained as the matrix element

$$M(t, \mathbf{Q}) = \int \exp(i\mathbf{Q} \cdot \mathbf{R}/\hbar) F(t, \mathbf{R}) d^2\mathbf{R}/(2\pi\hbar)^2 \quad (5)$$

where

$$F(t, \mathbf{R}) = \frac{1}{V} \int \psi(t, \mathbf{r}_0, \mathbf{r}_1, \dots) \psi^*(t, \mathbf{r}_0 + \mathbf{R}, \mathbf{r}_1, \dots) \prod_{k \geq 0} d^3\mathbf{r}_k$$

and V is the plasma volume.

Expression (5) can be significantly simplified for the case under consideration. The test particle affects only plasma particles in the interaction sphere $|\delta\mathbf{r}_{0,j}| < \lambda$, for which two-particle correlations among plasma particles are small owing to $T \gg e^2 n^{1/3}$. Aiming deliberately for calculations with logarithmic accuracy, we can omit the integration over $|\delta\mathbf{r}_{0,j}| > \lambda$ and use the method developed in [4]. We find $F(t, \mathbf{R}) = F_e(t, \mathbf{R})F_i(t, \mathbf{R})$ where $F_e(t, \mathbf{R}) = \exp(-f_e(t, \mathbf{R}))$,

$$f_e = 2N \int \sin^2 \left[\frac{\alpha}{4} (g(t, \mathbf{r}_0 + \mathbf{R}) - g(t, \mathbf{r}_0)) \right] \frac{d^3\mathbf{r}_0}{\lambda^3}, \quad (6)$$

$$g = \int_{-v_0 t}^{v_0 t} V_0(x_0 + \zeta/2 - v_0 t, y_0 + Y, z_0 + Z) d\zeta, \quad (7)$$

$N = n\lambda^3$, $\alpha = Z_0 e^2 / \hbar v_0$, $\mathbf{r}_0 = (x_0, y_0, z_0)$, $V_0(\mathbf{r}_0) = 1/|\mathbf{r}_0|$ for $|\mathbf{r}_0| < \lambda$ and $V_0 = 0$ for $|\mathbf{r}_0| > \lambda$. In the \mathbf{r}_0 -integration, the domain $\min((y_0 + Y)^2 + (z_0 + Z)^2, y_0^2 + z_0^2) < r_{cl}^2 = (Z_0 e^2 / m_e v_0^2)^2$ is excluded for reasons discussed above. The ion function F_i has the same structure as F_e and is simply obtained by substituting ion parameters. M is the convolution of M_e and M_i , where

$$M_{e,i}(t, \mathbf{Q}) = \int \exp(i\mathbf{Q} \cdot \mathbf{R}/\hbar) F_{e,i}(t, \mathbf{R}) d^2\mathbf{R}/(2\pi\hbar)^2$$

are the transverse momentum distributions due to the electron-projectile and ion-projectile interaction. In the following, most of the discussion is restricted to M_e .

Let us discuss the structure of Eqs. (6),(7), which are presented here for the first time. The detailed analysis is quite intricate, and here we give only the main results without derivation. We observe that only small enough f_e can contribute to M and that therefore, owing to the large multiplier N in Eq. (6), the \sin^2 -term needs to be small and can be expanded. Then M depends essentially on the parameter combination $\alpha^2 N$ only; more rigorous analysis gives $\gamma = \alpha^2 N \ln N$. The

quantum regime is restricted to $\gamma < 1$, while the classical regime is found for $\gamma > 1$ and will be discussed first. Evaluating Eq. (6) in the limit of very small R , one finds $f_e(\mathbf{R}) = \nu t \ln(\lambda m_e v_0^2 / Z_0 e^2) (\mathbf{R}/\hbar)^2$ with $\nu = 2\pi n Z_0^2 e^4 / v_0$. This is the relevant region in the Fourier integral of M_e for large enough time t ($t_1 \ll t < t_c$, see below). The function $F_e(\mathbf{R})$ is then a Gaussian, and M_e can be easily calculated. Setting $F_i = 1$, we obtain $\langle Q^2 \rangle_e = \int \mathbf{Q}^2 M_e(t, \mathbf{Q}) d^2\mathbf{Q} = 4\nu t L_{cl}$ and recover the classical Coulomb logarithm $L_{cl} = \ln(\lambda m_e v_0^2 / Z_0 e^2)$. The important new result here is that it applies to the whole region $\gamma > 1$ and not just to $\alpha > 1$.

It should be noticed, however, that the function $f_e(\mathbf{R}) = \nu t \ln(\lambda/\tilde{R}) (\mathbf{R}/\hbar)^2$ is more complicated in general and contains a factor $\ln \tilde{R}$ for larger radii, where $\tilde{R} = \max(\alpha|\mathbf{R}|, \alpha\hbar/m_e v_0)$ for $\alpha > 1$ and $\tilde{R} = \max(|\mathbf{R}|, \alpha\hbar/m_e v_0)$ for $\alpha < 1$. For short times, just somewhat larger than λ/v_0 , this logarithmic factor modifies the Gaussian character of $M_e(t, \mathbf{Q})$, giving it a power-law tail at high $Q = |\mathbf{Q}|$. We then obtain

$$M(t, \mathbf{Q}) = \exp(-Q^2/2p_0^2)/(2\pi p_0^2) \quad (8)$$

for $Q^2 < 2p_0^2 \ln \Lambda$ and

$$M(t, \mathbf{Q}) = 2p_0^2/(\pi\Lambda Q^4) \quad (9)$$

for $2p_0^2 \ln \Lambda < Q^2 < (2m_e v_0)^2$, where Λ is a solution of $\Lambda = \ln(2\pi\alpha_1 n \Lambda^2 v_0 t) \gg 1$, $\alpha_1 = \min(1, \alpha)$ and $p_0^2 = \nu \Lambda t$. Physically, the Gaussian distribution at small Q corresponds to small angle scattering and the power-law tail to close collisions with large momentum transfer. The tail is obtained only as long as $t < t_1 = 2m_e^2 v_0^2 / \nu \Lambda \ln \Lambda$, such that $2p_0^2 \ln \Lambda < (2m_e v_0)^2$. For longer times, small angle scattering dominates both small and large Q regions and the tail disappears.

We have checked the occurrence of this power-law tail by molecular dynamics (MD) simulations. We consider a test particle with $v_0 \gg v_{th}$ scattered completely classically in a finite plasma volume, having dimensions l of the order of the screening length. The simulation has been performed for a model case with $N = 80$ and $\alpha = 1.9$, just feasible on a modern PC. Results are plotted in Fig. 2 for time $t = 2l/v_0 < t_1$. The histogram presenting the MD results is in best agreement with the present theory (solid curve), clearly showing the power-law tail at high momenta. For comparison, also the purely Gaussian distribution obtained from the Landau collision integral is given as dashed line. Details of these simulations are outlined in the caption. Here we should make it clear that the power law tail originating from close collisions is obtained in nearly identical form within the binary collision approach, as it was shown by Landau [8] and Vavilov [9]. The present theory differs for small-angle scattering and therefore in the Gaussian part of $M(t, Q)$. To show the difference quantitatively, we have also solved the kinetic equation used in [8, 9]. The result can be written in a form equivalent to Eq. (5) with the function f_e now given approximately by $f_e^{(b)} = \nu t \ln(\alpha_1 \lambda / \tilde{R}) (\mathbf{R}/\hbar)^2$,

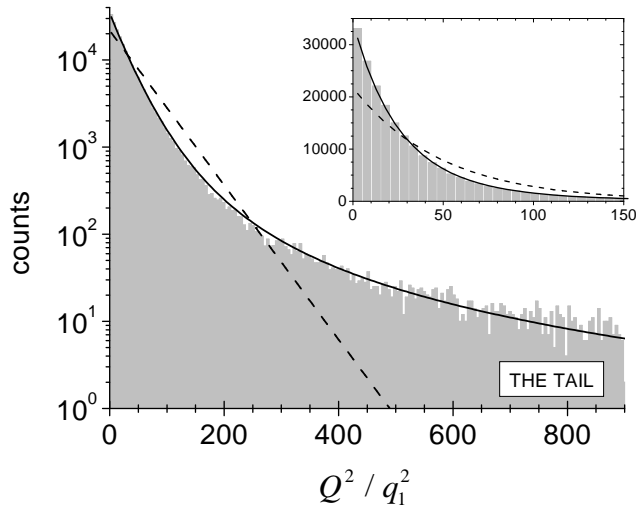


FIG. 2: Comparison between MD simulation (histogram), present theory (solid line), and predictions of the traditional diffusion approximation (dashed line); $\pi M(t, Q)$ is plotted versus Q^2/q_1^2 for time $t = 2l/v_0$, $l = 7.239 \times 10^{-6}$ cm, velocity of test particle $v_0 = 2.297 \times 10^8$ cm/s, and $q_1^2 = 2\pi n Z_0^2 e^4 t/v_0$. The insert shows the same plot, but with linear scale and zoomed to low Q . The simulation assumes an equal number of randomly distributed, fixed Coulomb centers of opposite charge $\pm e$ and densities $n_+ = n_- = n = 1.054 \times 10^{17}$ cm $^{-3}$; the cold plasma limit is chosen with thermal velocity $v_{th} \ll v_0$. The plasma volume is taken as $V = 6l \times 2l \times 2l$ with the test particle ($Z_0 = 2$, $m_0 = m_e$) moving along the central axis in x -direction and starting at a distance $2l$ from the surface. The trajectory of the test particle, interacting with all Coulomb centers, is obtained by solving the classical equation of motion by a second-order scheme with an adaptive time step. The histogram corresponds to 2.06×10^5 independent trials. The solid line has been obtained numerically from Eqs.(6)–(7) with $F_i = F_e = \exp(-f_e)$. The screening length is set to $\lambda = l$ such that the finite plasma volume seen by the test particle in this model simulation just mimics the physically screened volume occurring in reality. The straight dashed line is the Landau collision integral prediction $M(t, Q) = \exp(-Q^2/Q_0^2)/(\pi Q_0^2)$ with $Q_0^2 = 8\pi e^4 Z_0^2 (n_+ + n_-) L_0 t/v_0$; $L_0 = 6.5$ is the classical Coulomb logarithm evaluated for the parameters of the simulation.

where $\tilde{R} = \max(\alpha|\mathbf{R}|, \alpha\hbar/m_e v_0)$ and $\alpha_1 = \min(1, \alpha)$. The effect of the present theory is that the Gaussian part grows more rapidly. This is consistent with enhanced small-angle scattering due to simultaneous interaction with many plasma particles.

We have seen in Fig.1 that the quantum limit ($\gamma < 1$) is relevant only in a marginal parameter region. Nevertheless, it is contained in M_e . For $\gamma < 1$, one can use first-order expansions of $F_e = 1 - f_e$ and of the \sin^2 -term in f_e to find, after some algebra, $M_e(t, \mathbf{Q}) = C(t)\delta(\mathbf{Q}) + \sigma(Q)nvt/(m_e v)^2$, where

$C(t) = 1 - nvt/(m_e v_0)^2 \int \sigma(Q) d^2\mathbf{Q}$ and $\sigma(Q) \approx r_{cl}^2 (2m_e v_0)^4 / (Q^2 + (\hbar/\lambda)^2)^2$ is the cross-section of the screened Coulomb potential. This leads to $\langle Q^2 \rangle_e = 4vtL_q$ and the quantum (Bethe) logarithm $L_q = \ln(\lambda m_e v_0/\hbar)$. This first-order Born result is obtained here for $\alpha N^{1/2} \ll 1$, but not for $\alpha < 1$ in general. This may be understood qualitatively looking at second-order processes. Consider the perturbation of the interaction of the test particle with a plasma particle j by another plasma particle k . This effect is small of order α^2 , but since for a plasma with long-range Coulomb forces N particles contribute to this second-order process, it can be neglected only if $\alpha^2 N < 1$.

Let us finally calculate the energy $\mathcal{E}(t) = \langle \psi | \hat{H}_p | \psi \rangle$ the plasma gains due to the energy loss of the test particle. Here

$$\hat{H}_p = \sum_{j \geq 1} \left(-\hbar^2 \Delta_j / (2m_j) + \sum_{k > j} U_{j,k} \right)$$

is the Hamiltonian of the plasma without the test particle [5] and $\psi(t, \mathbf{r}_0, \mathbf{r}_1, \dots)$ the full wavefunction. Making use of the same approximations as in the derivation of Eq. (5), straightforward algebra leads to $d\mathcal{E}/dt = \langle Q^2 \rangle_e / 2m_e + \langle Q^2 \rangle_i / 2m_i$, where the first term is the contribution from plasma electrons with mass m_e and the second from ions with mass m_i . The corresponding electron part of the stopping power is then found in the standard form

$$\frac{dE}{dx} = -\frac{1}{v_0} \frac{d\mathcal{E}}{dt} = -\frac{4\pi n e^4 Z_0^2}{m_e v_0^2} L,$$

but now with $L = L_{cl}$ for $\gamma > 1$ and $L = L_q$ for $\gamma < 1$.

In conclusion, it has been shown that the theory of Coulomb scattering in dilute plasma needs revision. Bohr's classical Coulomb logarithm L_{cl} is found to apply for $\alpha\sqrt{N} > 1$ rather than $\alpha > 1$, and this covers most of the density-temperature plane, relevant to practical applications. This result calls for experimental verification. We propose to measure energy loss of fully stripped ions in carefully characterized, fully ionized plasma layers. The parametrically different dependence of L_{cl} and L_q on ion charge Z_0 and velocity v_0 should allow for a clear distinction.

Acknowledgments

The authors acknowledge controversial discussions with M. Basko and G. Maynard. This work was supported by Bundesministerium für Forschung und Technologie, Bonn and Counsel for the Support of Leading Russian Scientific Schools (Grant No. SS-2045.2003.2).

-
- [1] N. Bohr, *The penetration of atomic particles through matter* Math.-Fys. Medd XVIII (1948) (reprinted in *Niels Bohr Collected Works*, J. Thorsen, Vol 8, Amsterdam, North-Holland, 1987, page 425.
- [2] V.I. Kogan, Sov. Phys. Doklady **5**, 1960 (1316).
- [3] D.V. Sivukhin, *Reviews of Plasma Physics*, Editor M.A. Leontovich, Vol. 4, 1966, page 93.
- [4] S.N. Gordienko, JETP Letters **70**, 1999 (583).
- [5] A.I. Larkin, Sov. Phys. JETP **60**, 1960 (186).
- [6] H.A. Bethe, *Annalen der Physik* **5**, 1930 (325).
- [7] L.D. Landau, E.M. Lifshitz, *Quantum Mechanics. Non-Relativistic Theory*, Vol. 3, Oxford, Pergamon Press, 1987, page 763.
- [8] L.D. Landau, *Journal of Physics* **4**, 1944 (201).
- [9] P.V. Vavilov, JETP **32**, 1957 (320).